Energy Materials

Supplementary Materials

"One stone-two birds": reviving waste-activated carbon for stable polysulfide shuttle-free room-temperature Na-S batteries

Chunwei Dong[1], Zhihua Han[1], Zhijiang Su[1], Yang Dong[1], Quanbin Chen[1], Guofeng He[1], Xiaojie Sun[1], Nannan Zhang[1,*], Qing Jiang[2,*], Xiangjun Pu[3,*]

[1]National Institute of Clean-and-Low-Carbon Energy, Beijing 102209, China.
[2]Key Laboratory of Automobile Materials, Ministry of Education, School of Materials Science and Engineering, Jilin University, Changchun 130022, Jilin, China.
[3]Institute for Carbon Neutrality, Wuhan University, Wuhan 430072, Hubei, China.

[*]**Correspondence to:** Dr. Nannan Zhang, National Institute of Clean-and-Low-Carbon Energy, Beijing 102209, China. E-mail: 20099643@ceic.com; Prof. Qing Jiang, Key Laboratory of Automobile Materials, Ministry of Education, School of Materials Science and Engineering, Jilin University, Changchun 130022, Jilin, China. E-mail: jiangq@jlu.edu.cn; Dr. Xiangjun Pu, Institute for Carbon Neutrality, Wuhan University, Wuhan 430072, Hubei, China. E-mail: joy_pu@whu.edu.cn

ORCID: Chunwei Dong (0009-0005-1762-0593)

The figures in the Supplementary Materials are original and without any copyright issues are involved.

EXPERIMENTAL PTOCEDURES

Fabrication of materials

Preparation of carbon-black sulfur (CB/S) composite material. After mixing the carbon-black and sublimed sulfur in a 3:7 ratio, place the mixture in a mortar and grind for 30 minutes. Then place the mixture in a magnetic boat, which is placed in a tube furnace, and kept at 155 ℃ under an argon atmosphere for 12 hours. After natural cooling to room temperature, sulfur-carbon composite material is obtained.

Preparation of Na_2S_6 solution. In an argon-filled glove box, S and Na_2S are added into 10 ml of tetraethylene glycol dimethyl ether solution at a molar ratio of 5:1. The mixture is then stirred at 50 ℃ until sulfur completely dissolves, forming a brown-red 0.5 mol/L Na_2S_6 solution. Further dilution of the solution is required before performing polysulfide permeation experiments and adsorption tests.

Visualized Na_2S_6 adsorption measurement. Take two clean small glass bottles, and place them into the glove box. Add equal volumes of Na_2S_6 solution to each bottle. One serves as the blank control, while another bottle is added with a certain amount of N-AC. After standing for six hours, observe the changes in the solution. The more transparent the solution, the stronger the adsorption capacity; conversely, the weaker the adsorption capacity.

Figure S1 Schematic diagram of GF@N-AC separator synthesis process.

The XRD patterns of sublimed sulfur (S), N-AC, and N-AC/S composites are shown in Figure S2. By comparison, it can be seen that the diffraction peaks of the S and N-AC/S samples match those of the standard card S (JCPDS 08-0247)[1, 2]. The diffraction peaks at 23.0°, 25.8°, and 27.6° are characteristic peaks of S, corresponding to its (222), (026), and (040) crystal planes, respectively, confirming the successful preparation of the composite material[3].

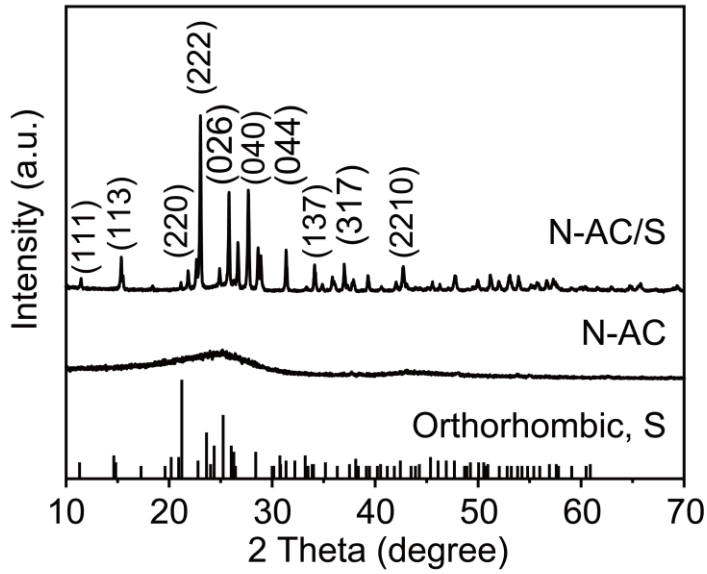

Figure S2 XRD patterns of N-AC and N-AC/S composites.

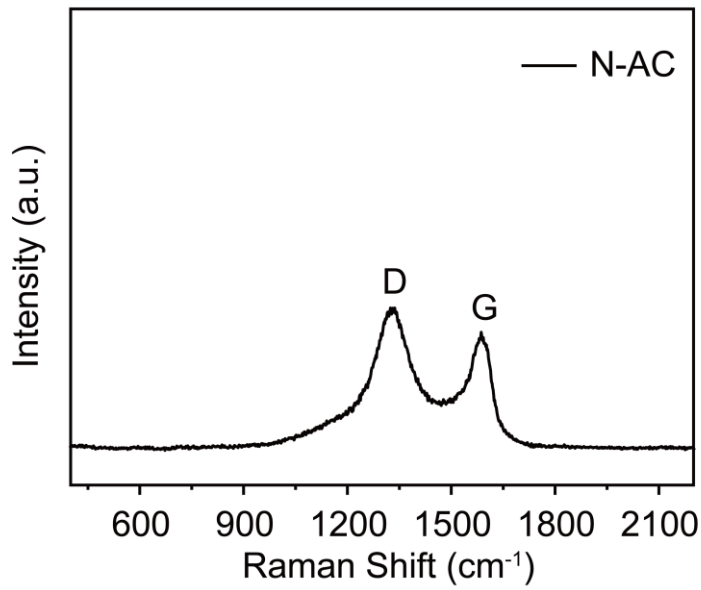

Figure S3 Raman spectrum of N-AC.

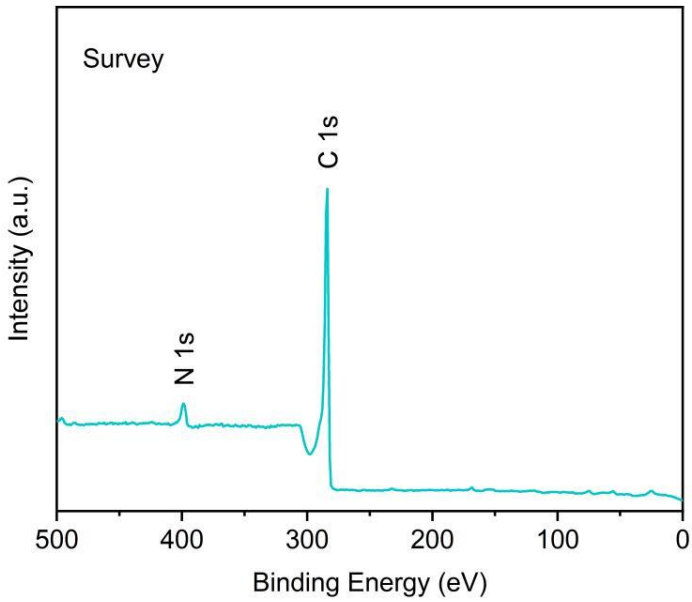

Figure S4 XPS survey spectrum of N-AC.

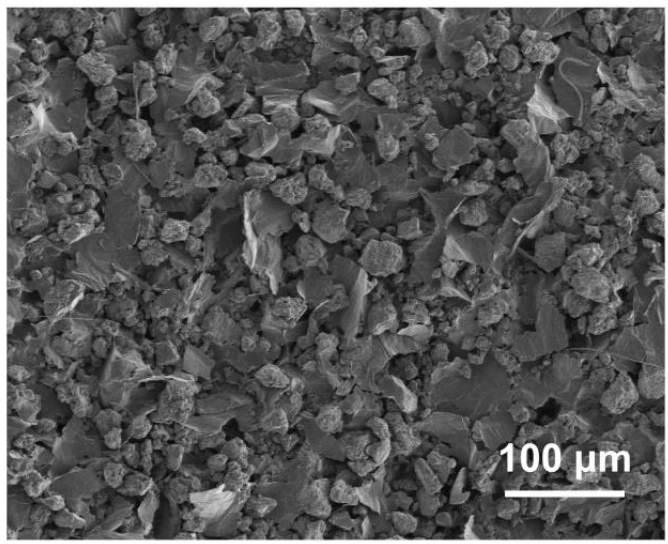

Figure S5 SEM images of the modified separator with N-AC.

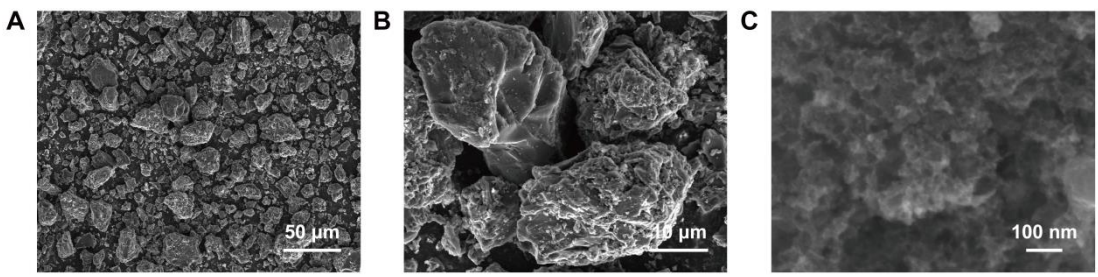

Figure S6 SEM images of N-AC at different magnifications.

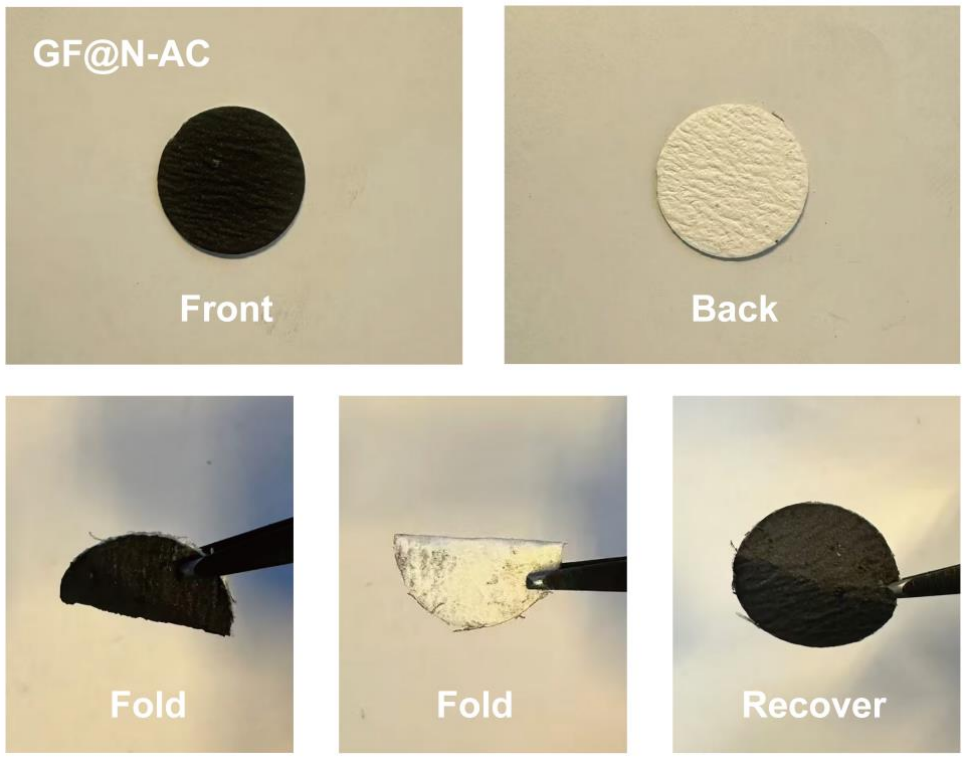

Figure S7 Digital photos of GF@N-AC separator.

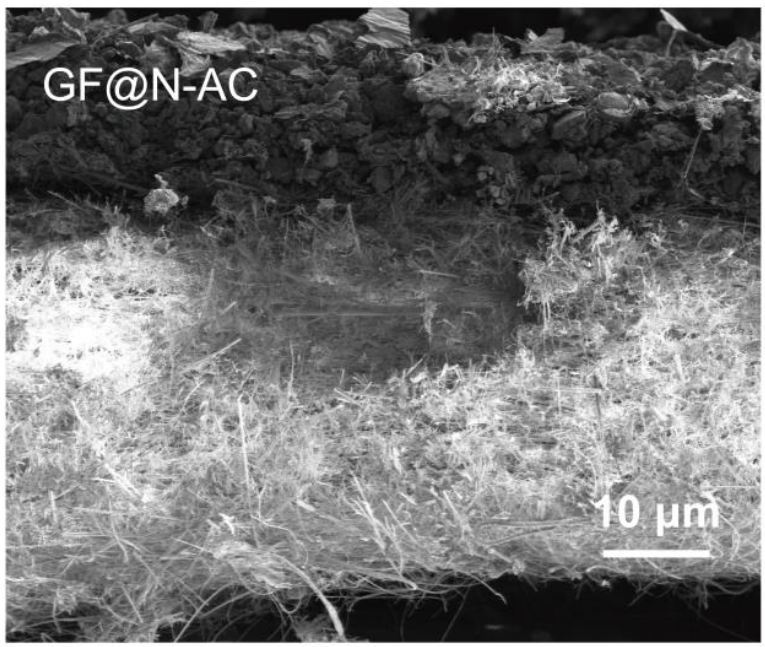

Figure S8 SEM image of GF@N-AC separator after folding.

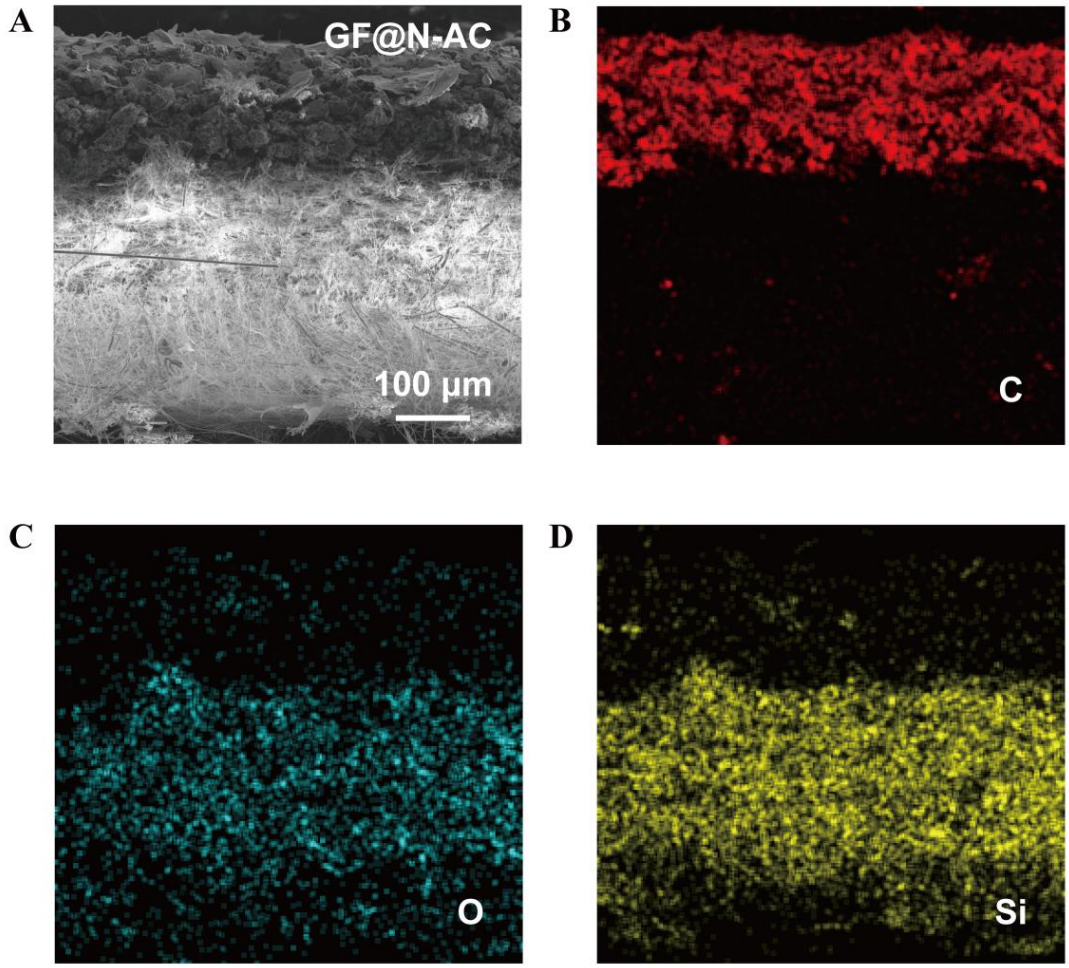

Figure S9 SEM and EDS elemental mapping images of GF@N-AC separator after folding.

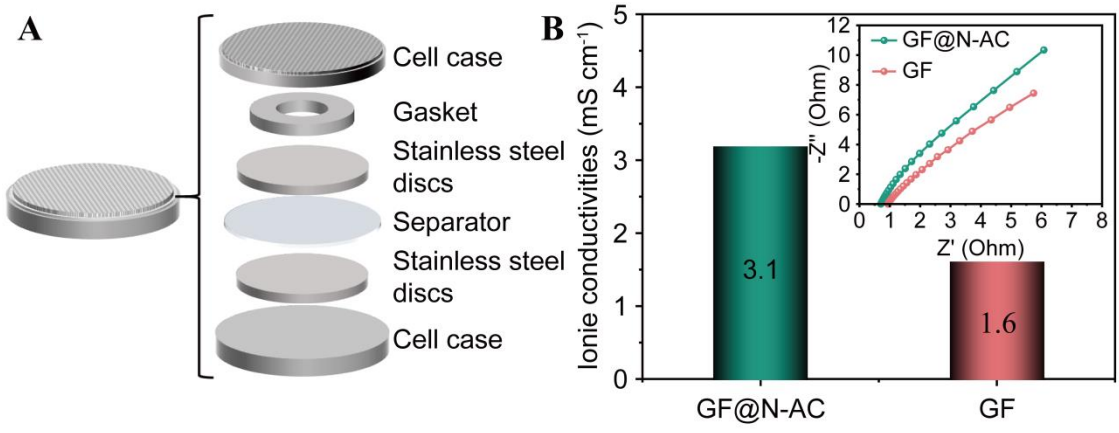

Figure S10 (A) Schematic diagram of the battery structure for testing ionic conductivity. (B) Ionic conductivity and Nyquist plots of GF separator and GF@N-AC separator.

For a preliminary analysis of the feasibility of GF@N-AC for room-temperature Na-S batteries, the ionic conductivity was assessed using a battery with the structure shown in Figure S10A (*J. Mater. Chem. A*, 2024, 12, 277-285; *J. Energy Storage*, 2025, 109, 115168). The ionic conductivity, σ, was calculated according to the following equation:

$$\sigma = \frac{d}{10 \times R \times A}$$

where d (μm), A (cm^2) and R (Ω) are the thickness, electrode contact area, and bulk resistance, which is determined by the intercept with the z-axis in the Nyquist plot (inset of Figure S10B). As a result, the ionic conductivity of the GF@N-AC separator is calculated to be 3.1 mS cm^{-1}, which is higher that of the GF separator (1.6 mS cm^{-1}). Hence the modification of commercial glass fiber (GF) separator with the porous nitrogen-doped waste activated carbon (N-AC) as a functional coating layer has no obstruction for Na^+ ions transport.

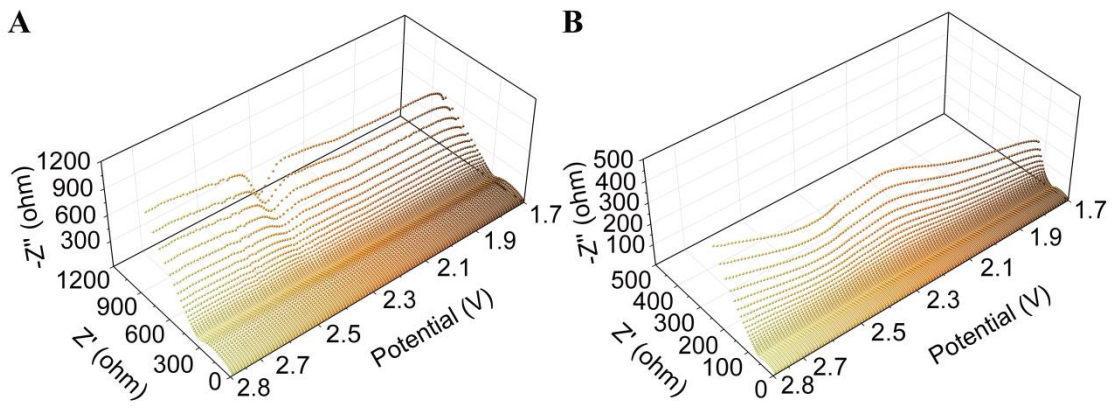

Figure S11 In situ electrochemical impedance spectra of GF separator (A) and GF@N-AC separator (B).

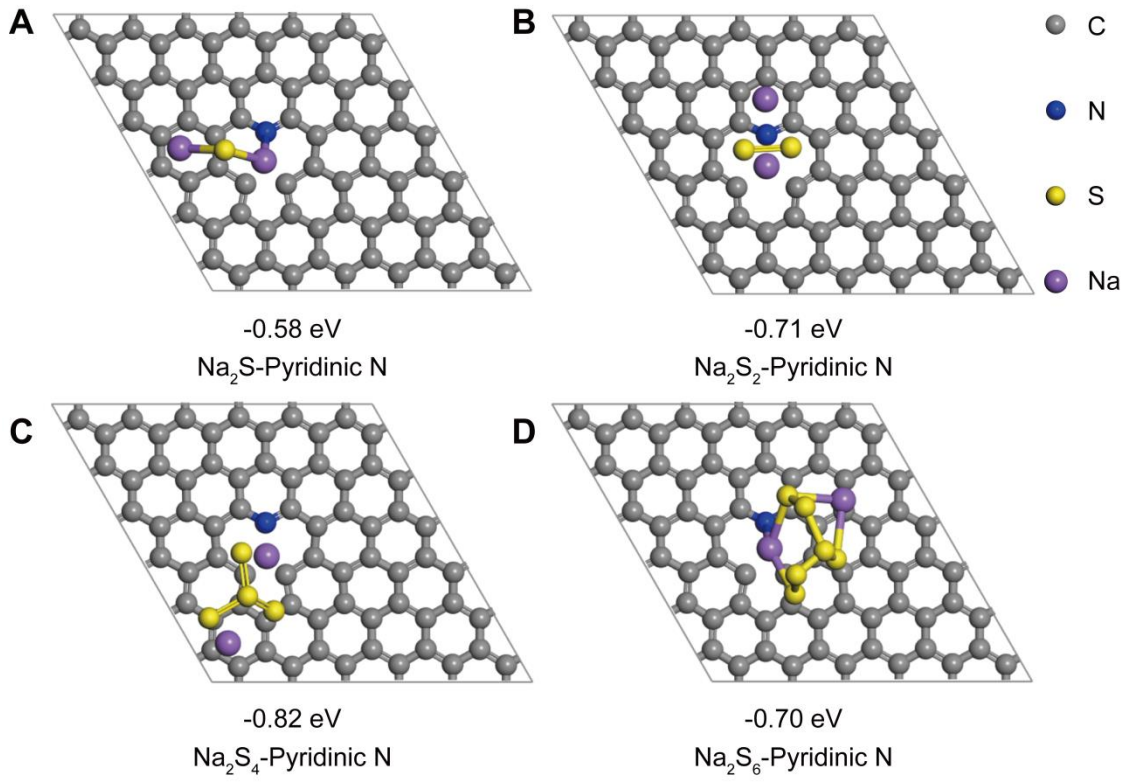

Figure S12 The optimized adsorption conformations of various sulfur species on pyridinic N-doped graphene layers (Top view)

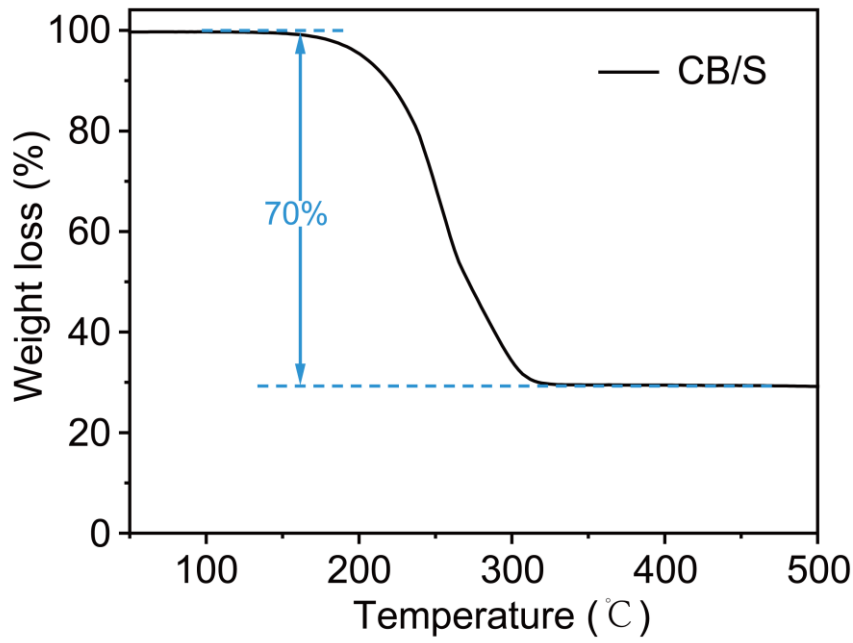

Figure S13 Thermogravimetric curve of CB/S composites.

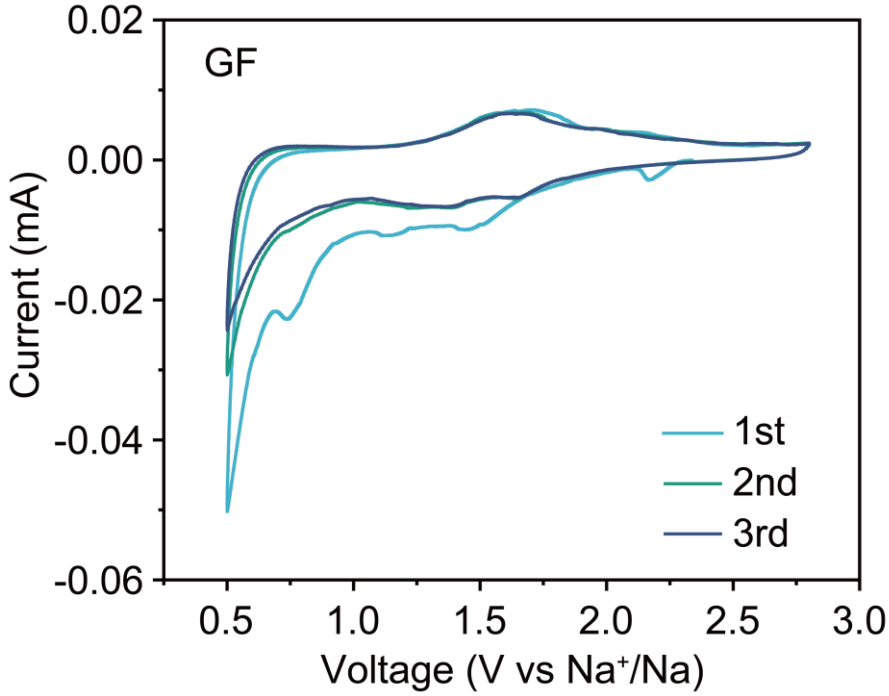

Figure S14 CV curves of cells with GF separator at 0.1 mV s^{-1}.

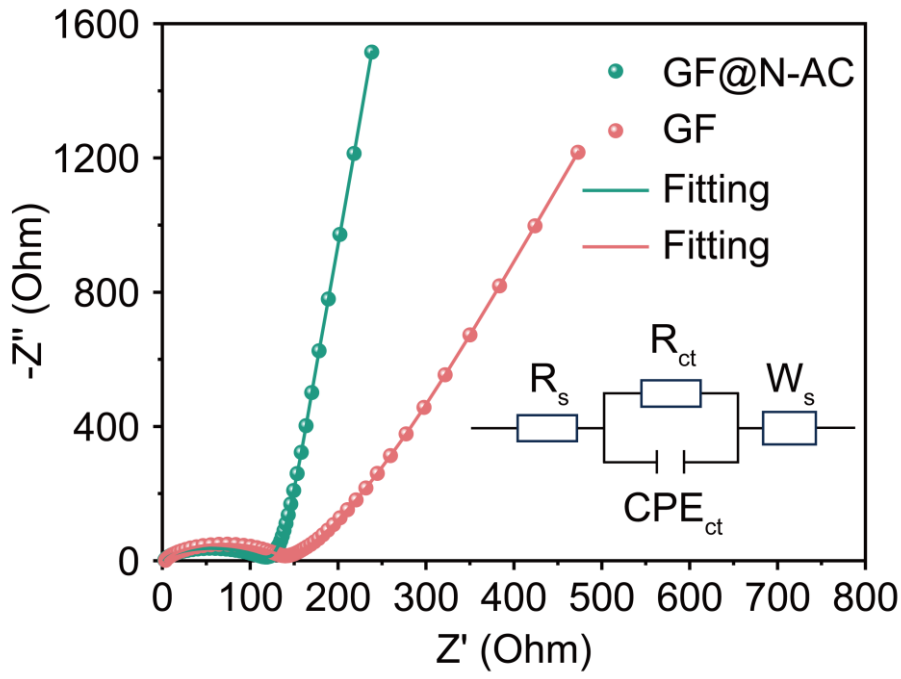

Figure S15 Nyquist plots of the GF@N-AC and GF separator and equivalent circuit model.

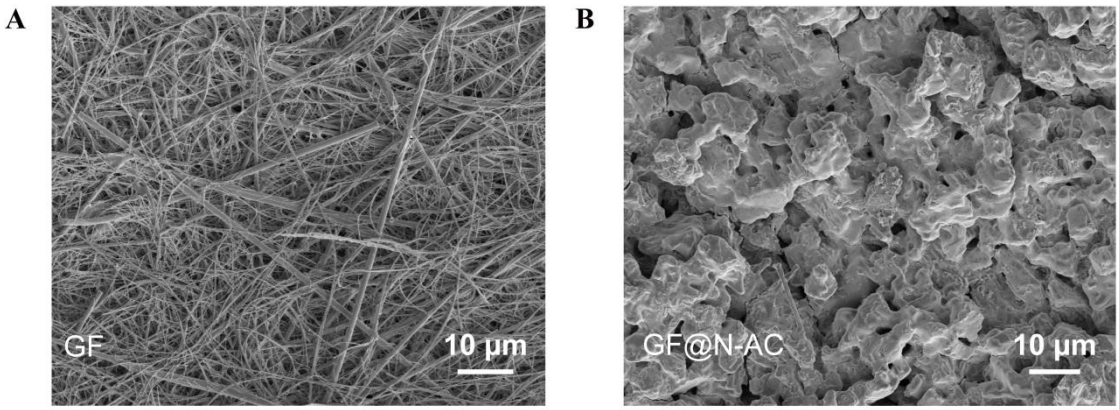

Figure S16 SEM images after 50 cycles of GF separator (A), and GF@N-AC separator (B).

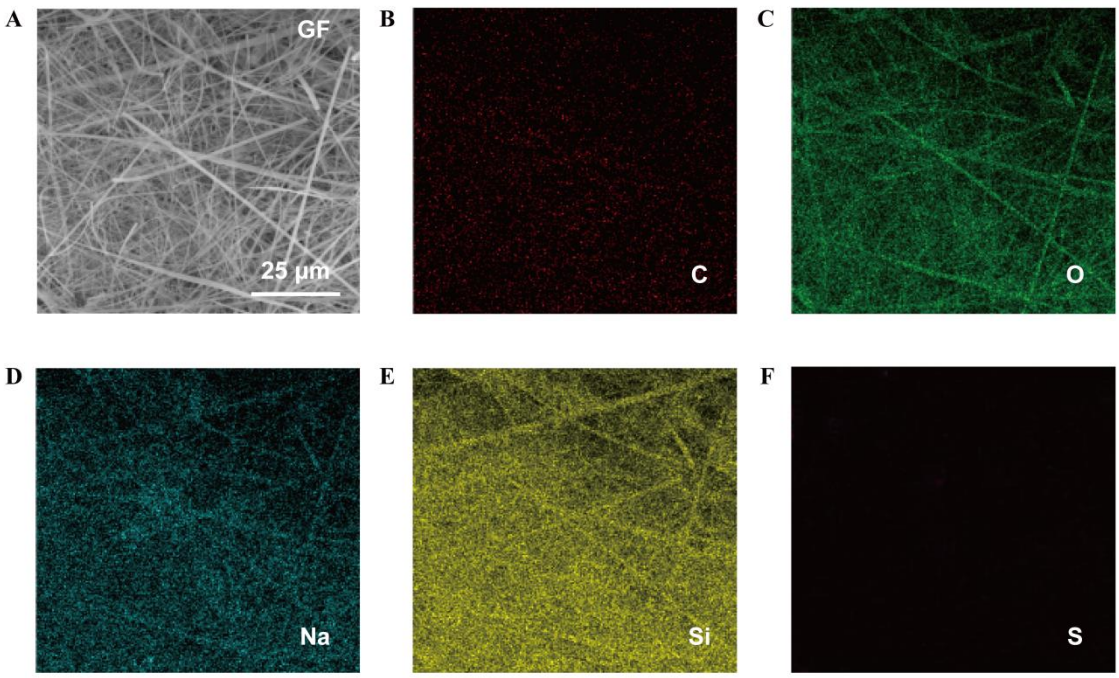

Figure S17 (A) SEM image of initial GF separator. (B-G) EDS elemental mappings of initial GF separator were obtained from SEM.

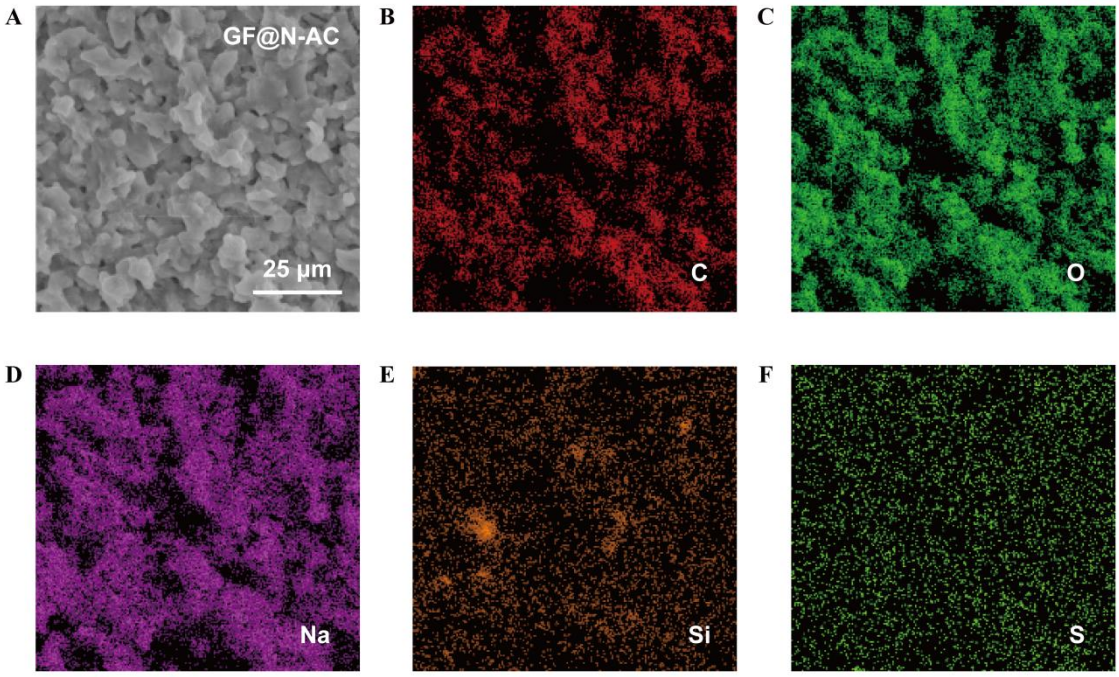

Figure S18 (A) SEM image of GF@N-AC separator. (B-G) EDS elemental mappings of GF@N-AC separator were obtained from SEM.

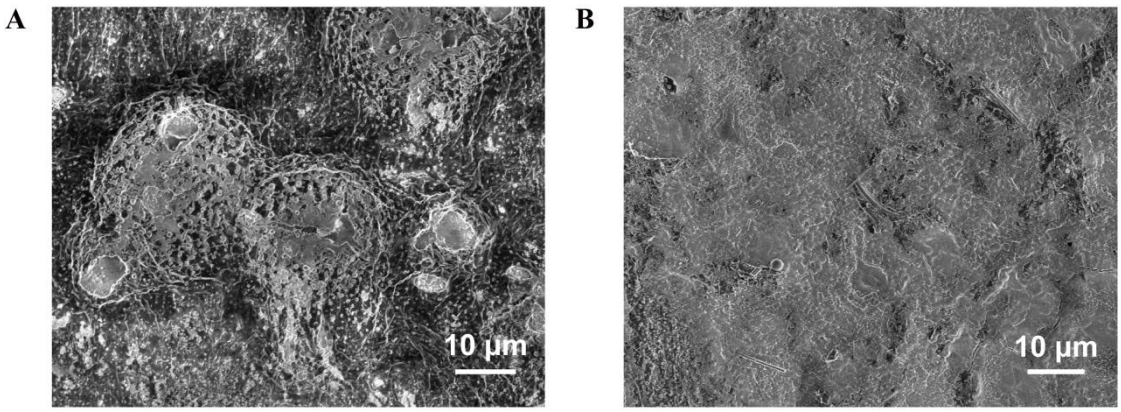

Figure S19 SEM images of Na metal anodes after 50 cycles paired with (A) GF separator, and (B) GF@N-AC separator.

As shown in Figure S16, after 50 cycles, the pure GF separator exhibits a relatively rough surface due to residual electrolyte and minor carbon black deposition, whereas the modified separator shows no obvious morphological change, with the coating layer remaining intact.

No sulfur signal is detected on the pure GF separator (Figure S17), however, EDS

analysis confirms the presence of sulfur on the modified separator, indicating effective adsorption of sodium polysulfides during cycling (Figure S18). This is further supported by SEM images of the sodium anodes (Figure S19), where a smooth surface is observed for the cell with the modified separator, while a much rougher morphology appears for the cell using the pristine GF separator. These results demonstrate that the modified separator effectively suppresses polysulfide shuttling and enhances cell performance.

Table S1. The content of different nitrogen species

N types	Pyridinic N	Pyrrolic N	Graphitic N	Oxidized-N
Content (%)	41.1	31.3	12.7	14.9

Table S2. Binding energy values of various NaPSs adsorbed on graphene, graphitic N, pyridinic N and Pyrrolic N

Types	Graphene	Graphitic N	Pyridinic N	Pyrrolic N
Na_2S	-0.34	-0.41	-0.58	-0.63
Na_2S_2	-0.45	-0.50	-0.71	-0.74
Na_2S_4	-0.60	-0.67	-0.82	-0.91
Na_2S_6	-0.55	-0.58	-0.70	-0.86

Table S3. The calculated R_s and R_{ct} of GF and GF@N-AC separator.

R types	R_s	R_{ct}
GF	2.771	120.6
GF@N-AC	1.916	103.4

References

1. Xu M, Zhu Q, Li Y, Gao Y, Sun N, Xu B. Atom-dominated relay catalysis of high-entropy MXene promotes cascade polysulfide conversion for lithium-sulfur batteries. *Energy Environ Sci* 2024;17:7735-7748.

2. Gao R, Zhang Q, Wang H, Wang F, Ren J, Wang X, Ma X, Wang R. Synergic effect of covalent and chemical sulfur fixation enhancing the immobilization-conversion of polysulfides in lithium-sulfur batteries. *J Energy Chem* 2023;79:1-11.

3. Li J, Chen C, Chen Y, Li Z, Xie W, Zhang X, Shao M, Wei M. Polysulfide confinement and highly efficient conversion on hierarchical mesoporous carbon nanosheets for Li-S batteries. *Adv Energy Mater* 2019;9:1901935.